

Supporting Information For

Synthesis, characterization and biological evaluation of mixed-ligand ruthenium(II) complexes for photodynamic therapy

Huaiyi Huang, Pingyu Zhang, Bole Yu, Chengzhi Jin, Liangnian Ji* and Hui Chao*

MOE Key Laboratory of Bioinorganic and Synthetic Chemistry, School of Chemistry and
Chemical Engineering, Sun Yat-Sen University, Guangzhou 510275, P. R. China.

E-mail: cesjln@mail.sysu.edu.cn; ceschh@mail.sysu.edu.cn

Content

Figure S1 ES-MS spectrum of ligand dpe.....	2
Figure S2 ¹ H NMR spectrum of ligand dpe.....	2
Figure S3 ES-MS spectrum of Ru1.....	3
Figure S4 ¹ H NMR spectrum of Ru1.....	3
Figure S5 ES-MS spectrum of Ru2.....	4
Figure S6 ¹ H NMR spectrum of Ru2.....	4
Figure S7 ES-MS spectrum of Ru3.....	5
Figure S8 ¹ H NMR spectrum of Ru3.....	5
Figure S9 Photostability of Ru1-Ru3 under continuous irradiation.....	6
Figure S10 Reactive oxygen species generated by Ru1 and Ru2 upon irradiation.....	7
Figure S11 UV-Vis spectra of Ru1-Ru3 by gradually increasing concentration.....	7
Figure S12 Changes in UV-Vis spectra of Ru1 and Ru2 upon adding CT-DNA.....	8
Figure S13 Ru(II) complexes inhibited DNA transcription.....	8
Figure S14 Colocalization images of Ru1-Ru3 with lysosome dye.....	9
Figure S15 Colocalization images of Ru1-Ru3 with mitochondria dye.....	9
Figure S16 Morphology changes and ROS generation in HepG2 cells.....	10
Figure S17 Stability of Ru1-Ru3 after irradiation detected by UV-Vis spectra.....	11
Figure S18 Plasma stability of Ru1-Ru3 detected by HPLC.....	12
Table S1 Crystal data and structure details of Ru1.....	13
Table S2 Selected bond lengths (Å) and angles (°) for Ru1.....	14
Table S3 Photophysical properties of Ru1-Ru3 in CH ₃ CN.....	14

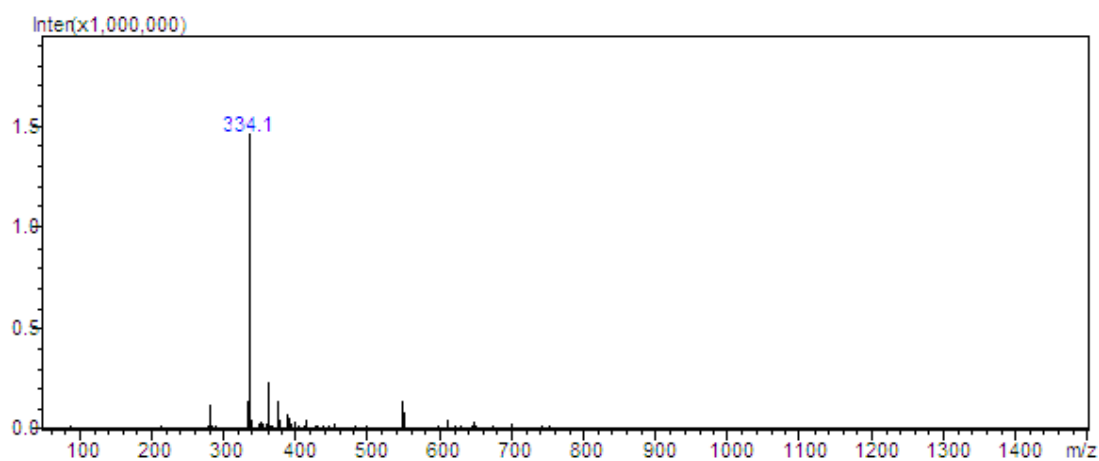


Figure S1 ES-MS (CHCl_3) spectrum of ligand dpe.

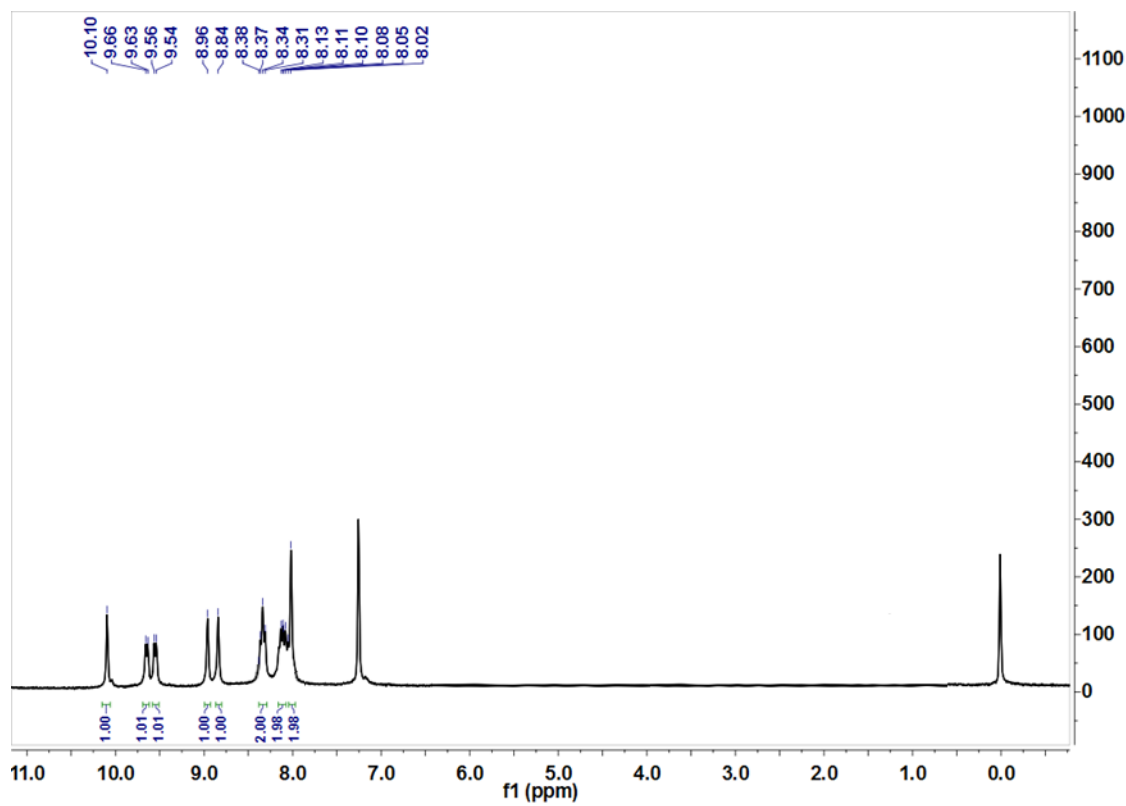


Figure S2 ^1H NMR spectrum (300 MHz, CDCl_3) of ligand dpe.

1

2

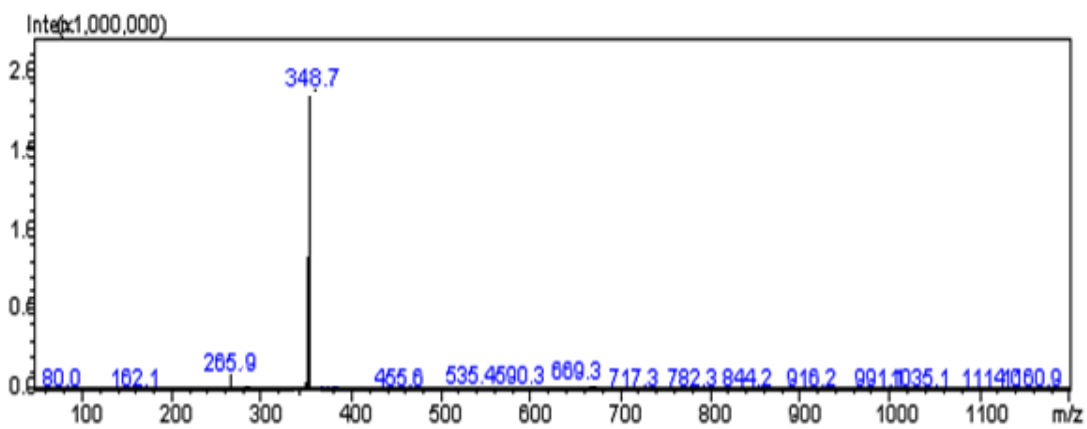


Figure S3 ES-MS (CH_3CN) spectrum of **Ru1**.

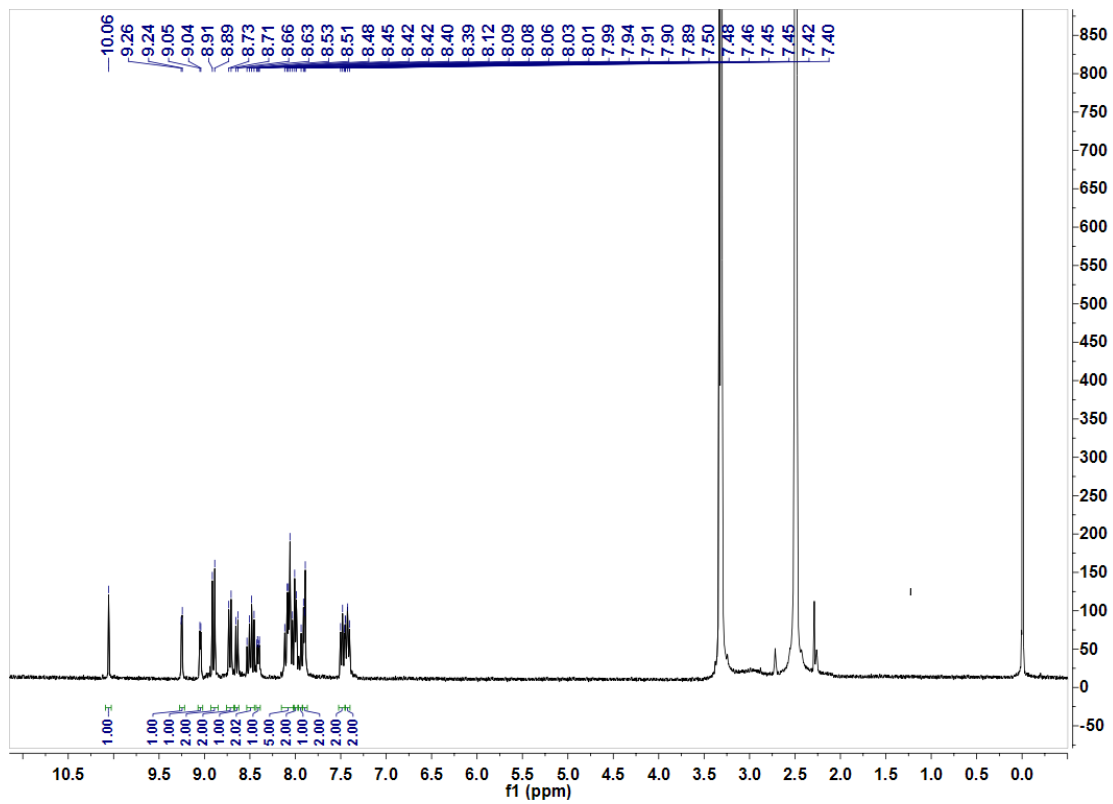


Figure S4 ^1H NMR spectrum (300 MHz, $\text{DMSO}-d_6$) of **Ru1**.

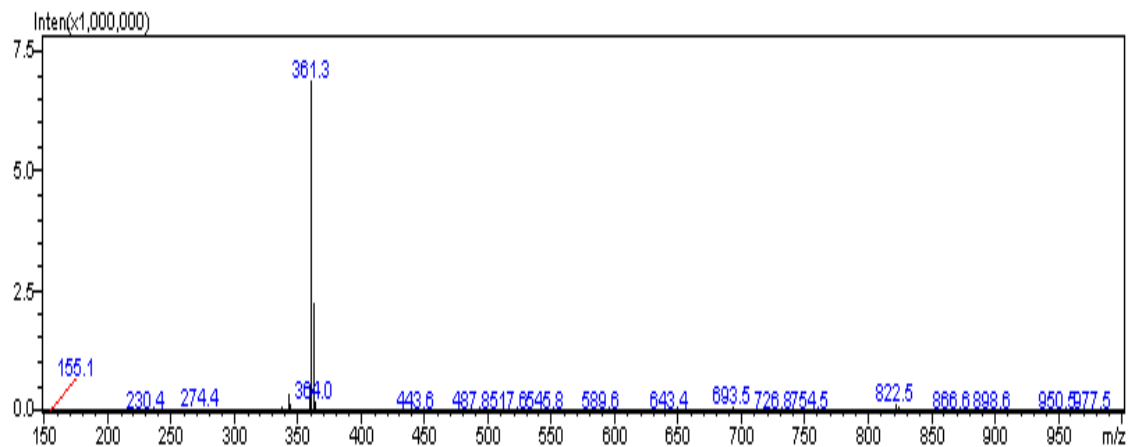


Figure S5 ES-MS (CH_3CN) spectrum of **Ru2**.

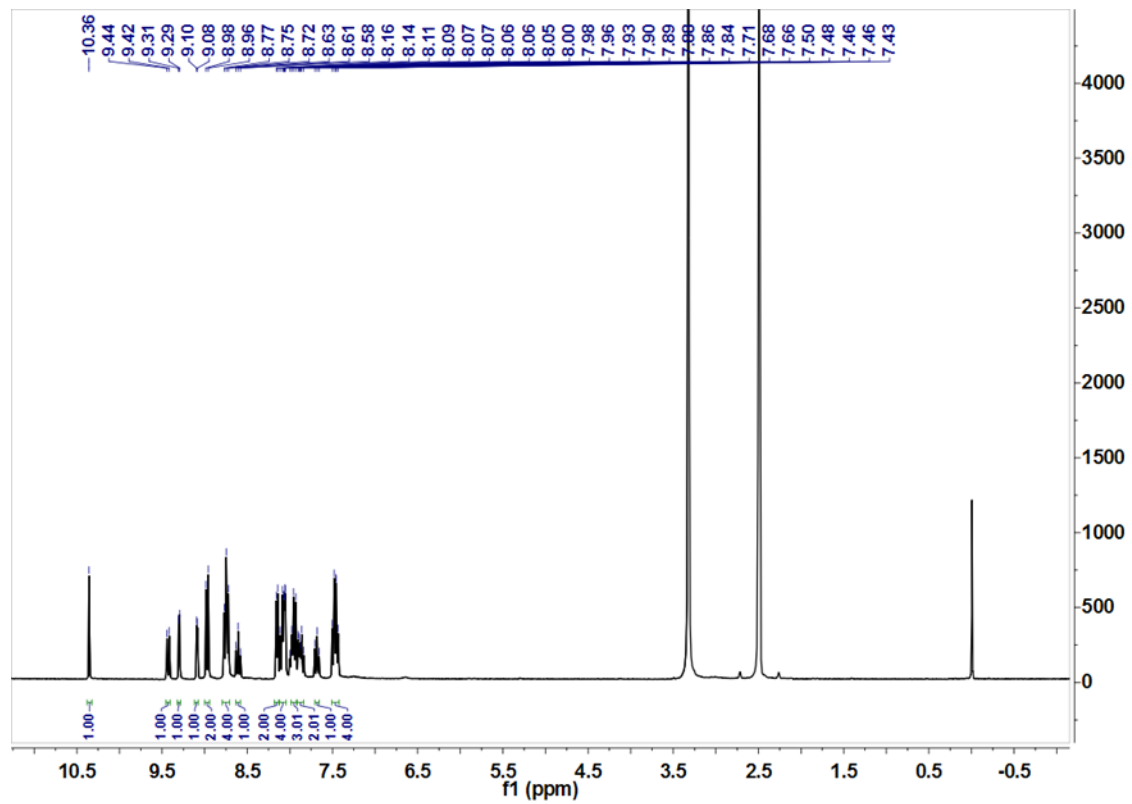


Figure S6 ^1H NMR spectrum (300 MHz, $\text{DMSO}-d_6$) of **Ru2**.

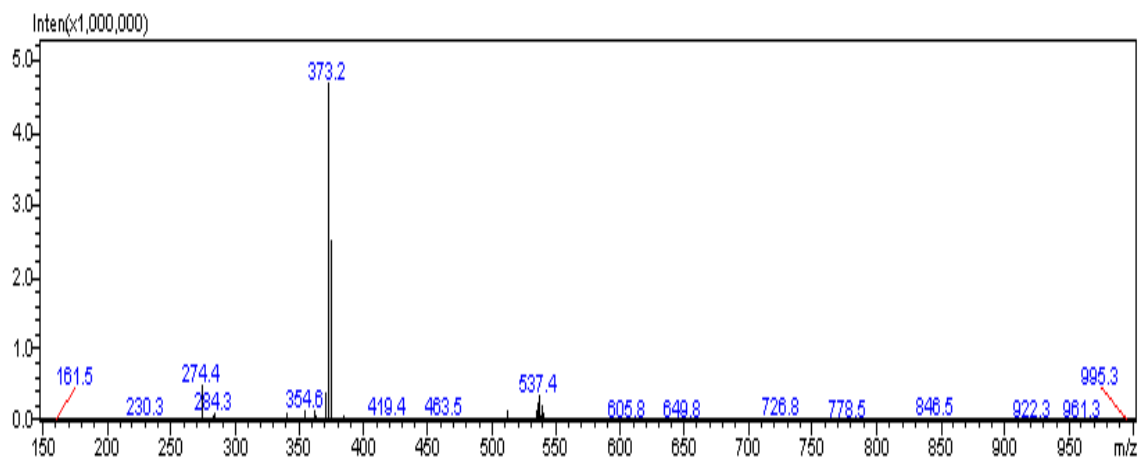
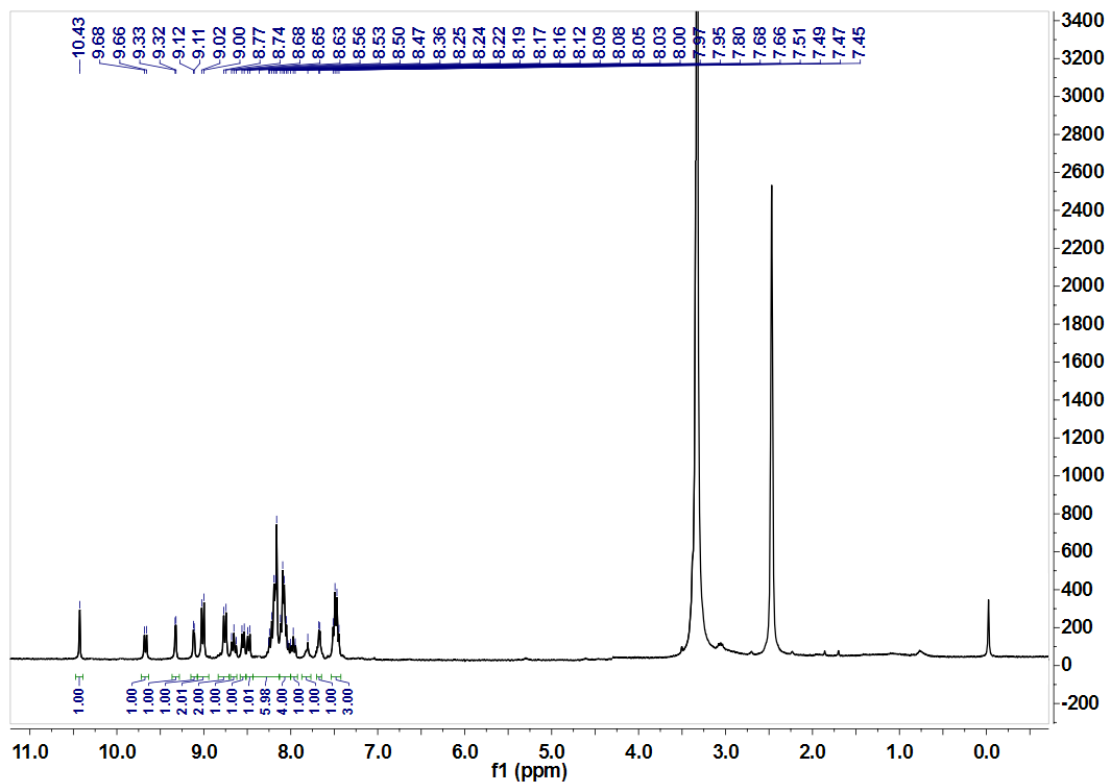


Figure S7 ES-MS (CH_3CN) spectrum of **Ru3**.



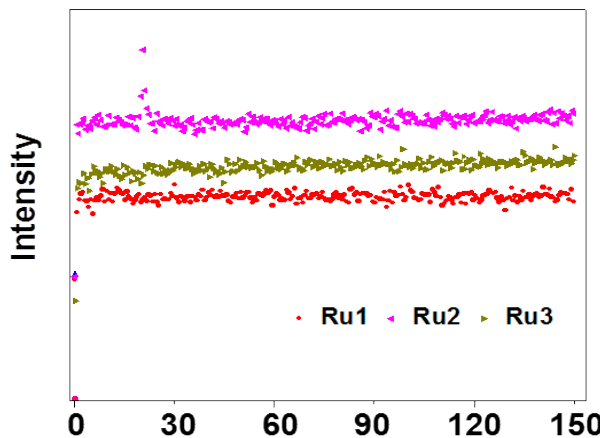


Figure S9 Photostability of **Ru1**-**Ru3** under continuous irradiation.

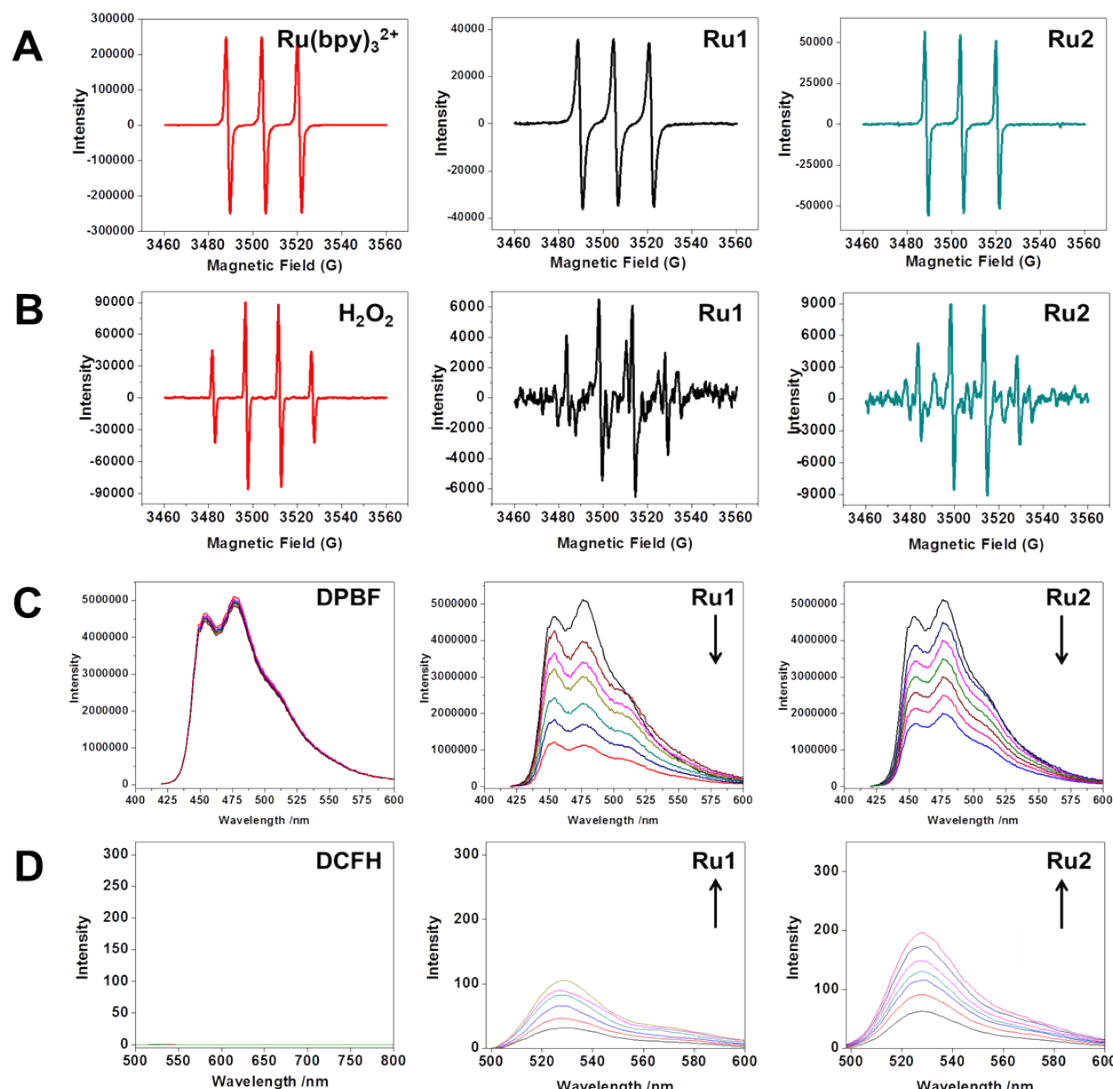


Figure S10 (A) ESR signals of $[\text{Ru}(\text{bpy})_3]^{2+}$ and **Ru1** and **Ru2** trapped by TEMP. (B) ESR signals of H_2O_2 and **Ru1** and **Ru2** trapped by DMPO. (C) Emission spectra of DPBF-**Ru1** and DPBF-**Ru2**. (D) Emission spectra changes of DCFH-**Ru1** and DCFH-**Ru2**.

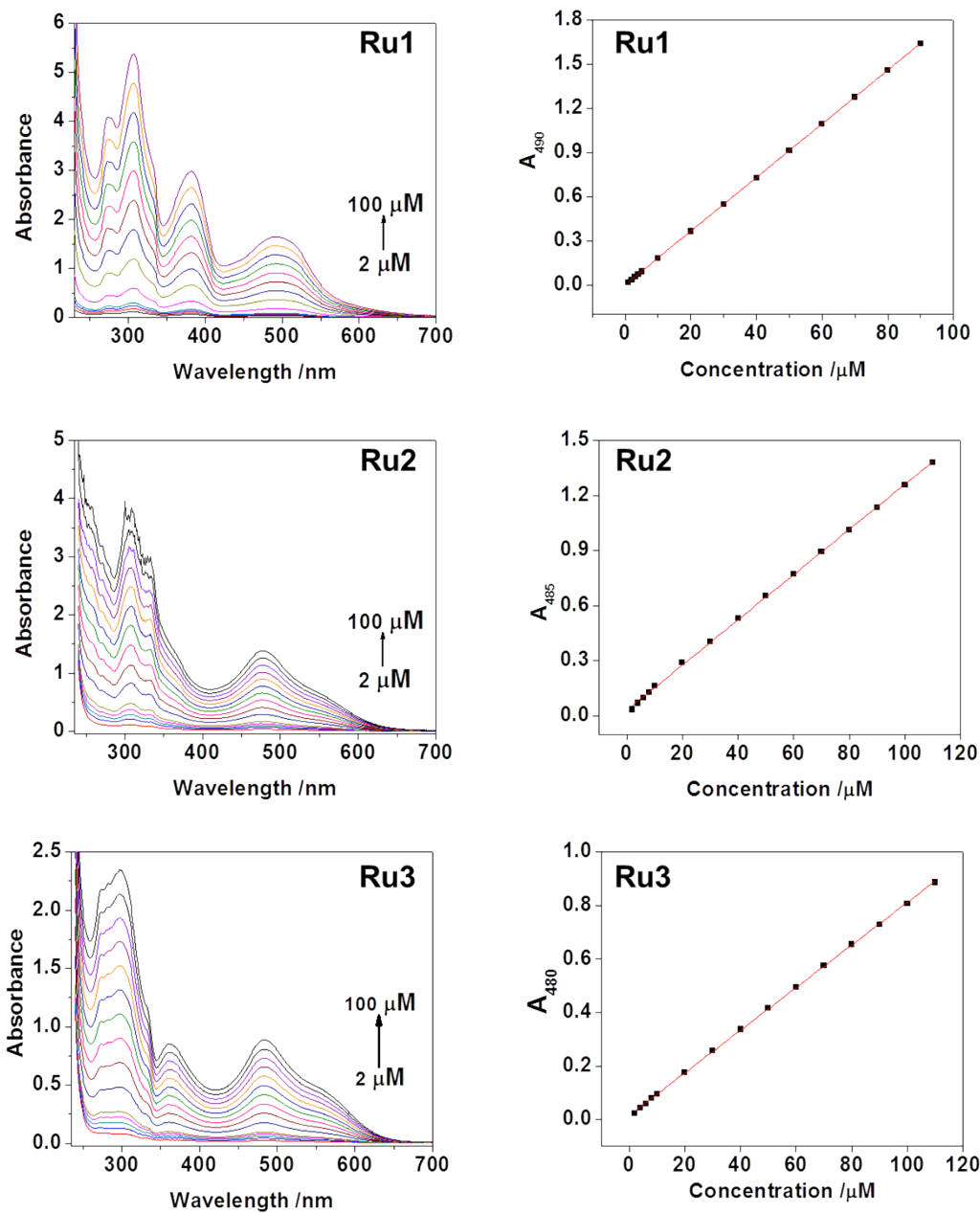


Figure S11 UV-vis spectra of **Ru1-Ru3** by gradually increasing concentration in Tris-HCl buffer (5 mM Tris, 50 mM NaCl, pH = 7.4).

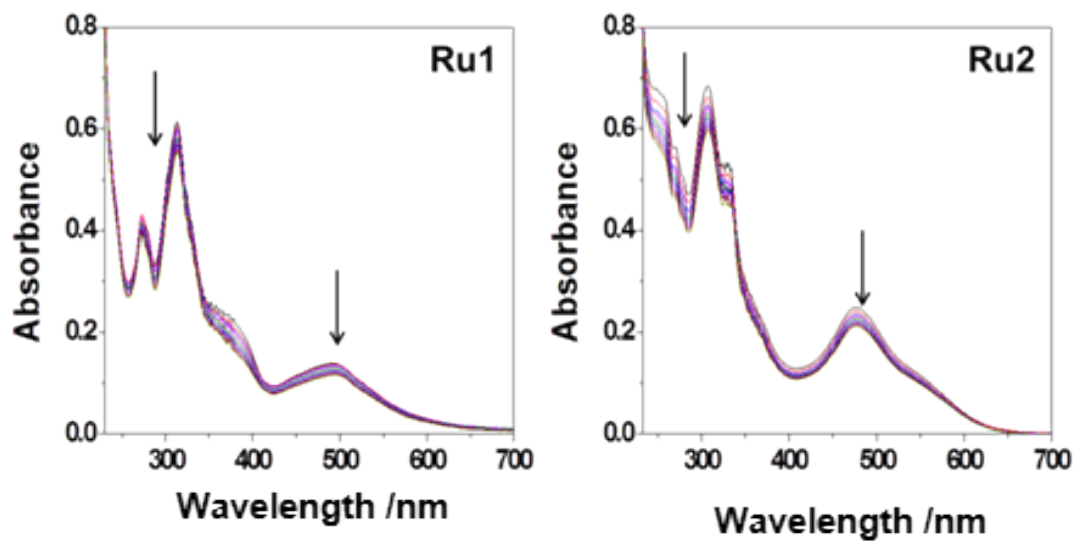


Figure S12 Changes in UV–Vis spectra of **Ru1** and **Ru2** upon adding CT–DNA;

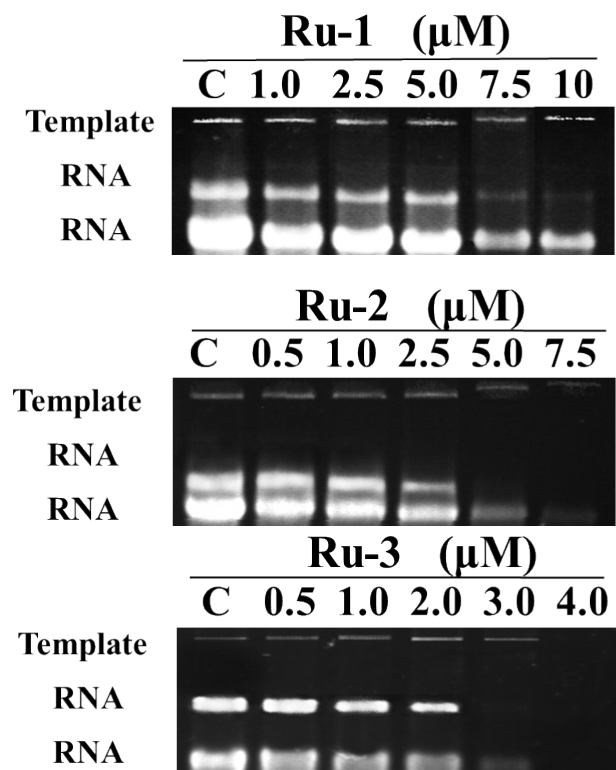


Figure S13 Ru(II) complexes inhibited RNA production during DNA transcription.

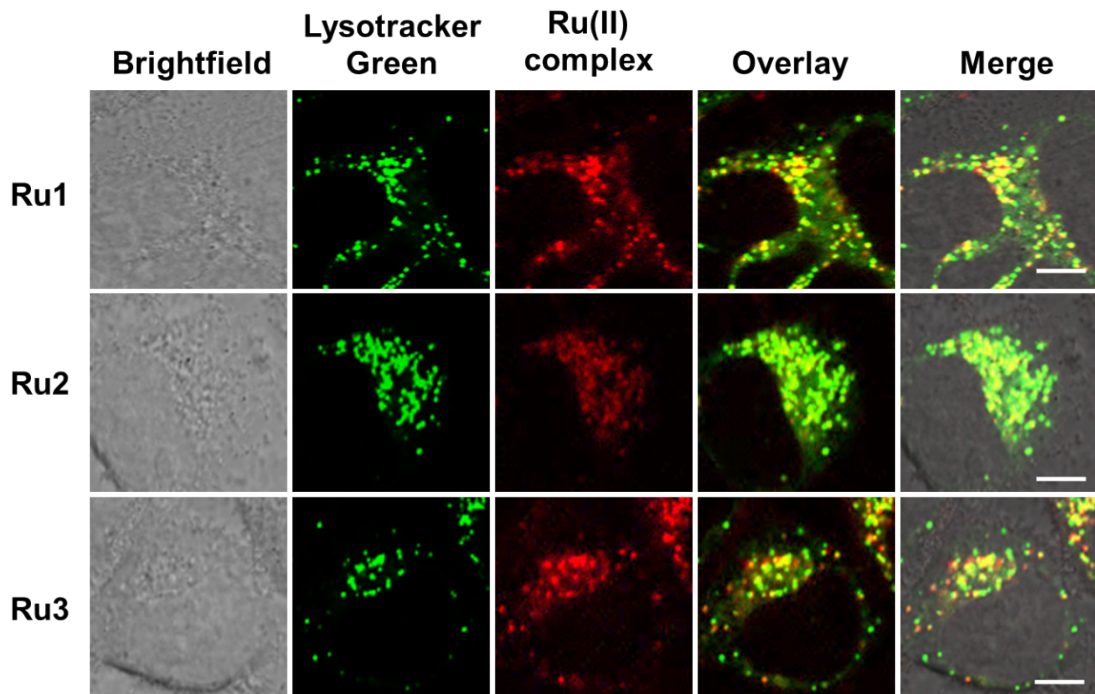


Figure S14 Colocalization images of Ru1–Ru3 with lysosome dye. Scale bars = 5 μ m.

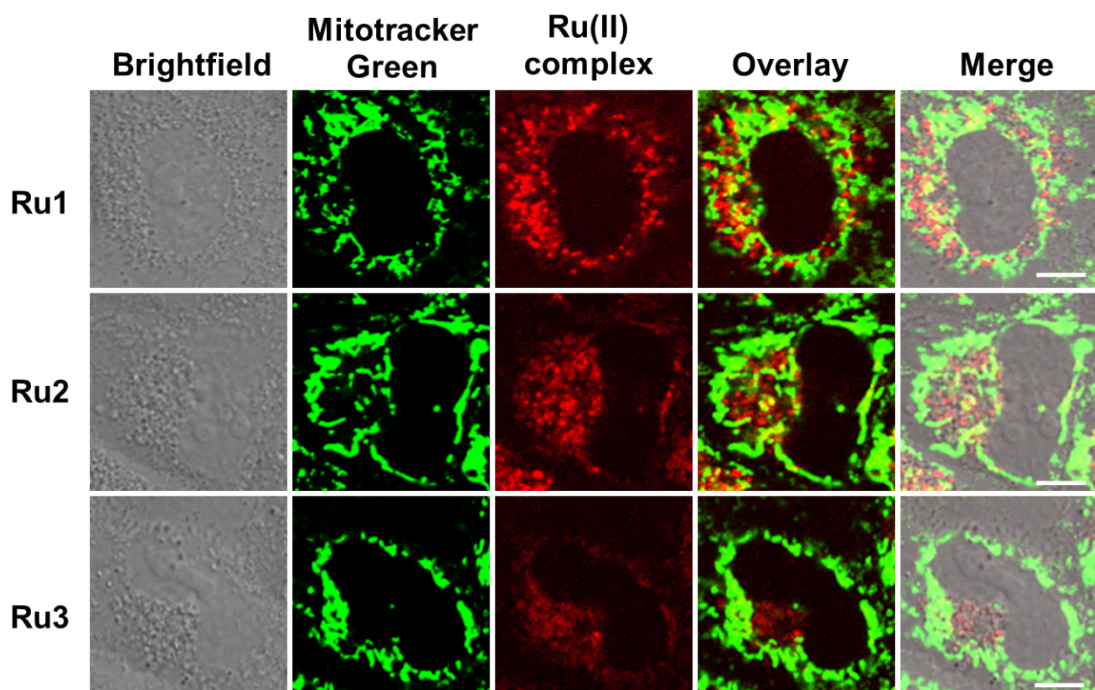


Figure S15 Colocalization images of Ru1–Ru3 with mitochondria dye. Scale bars = 5 μ m.

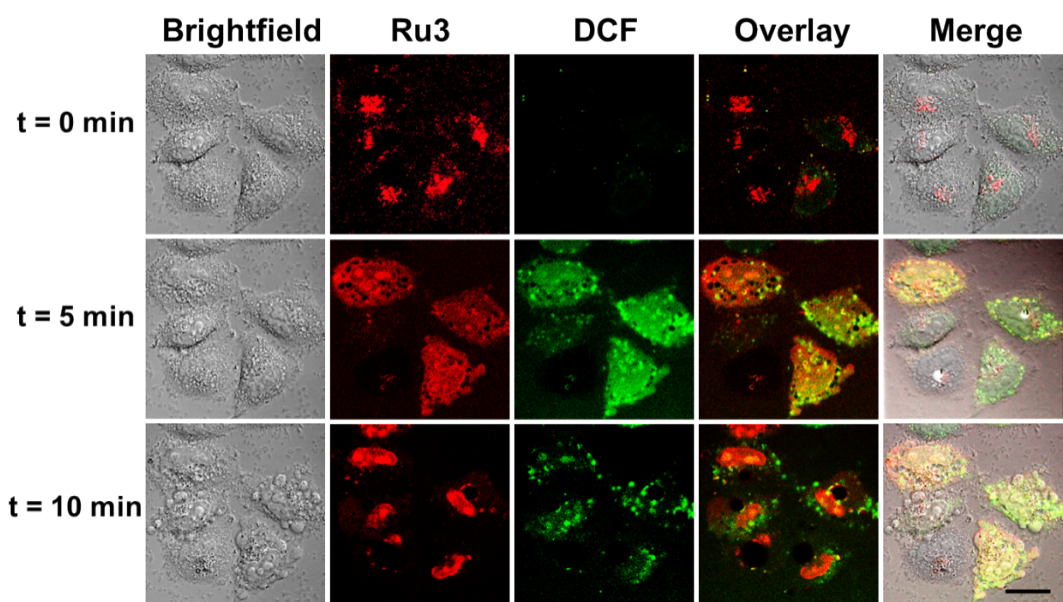
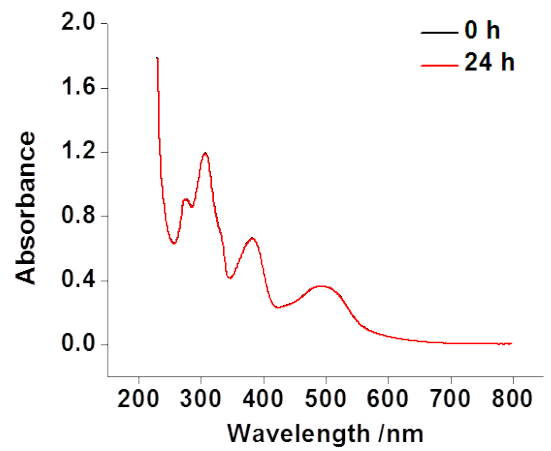
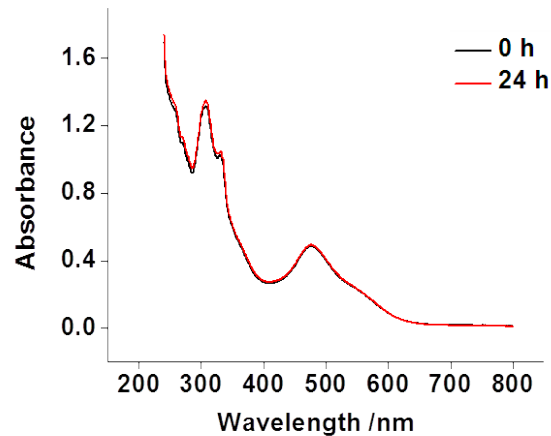


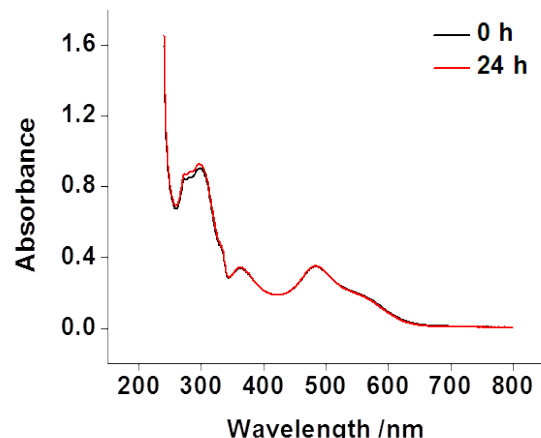
Figure S16 Morphology changes and cellular ROS generation within HepG2 cells incubated with **Ru3** (2.0 μ M) at different time. Scale bars = 10 μ m.



Ru1



Ru2



Ru3

Figure S17 Photostability of Ru1-3 (10 μ M) detected by UV-Vis spectra in Tris-HCl buffer (5 mM Tris, 50 mM NaCl, pH = 7.4).

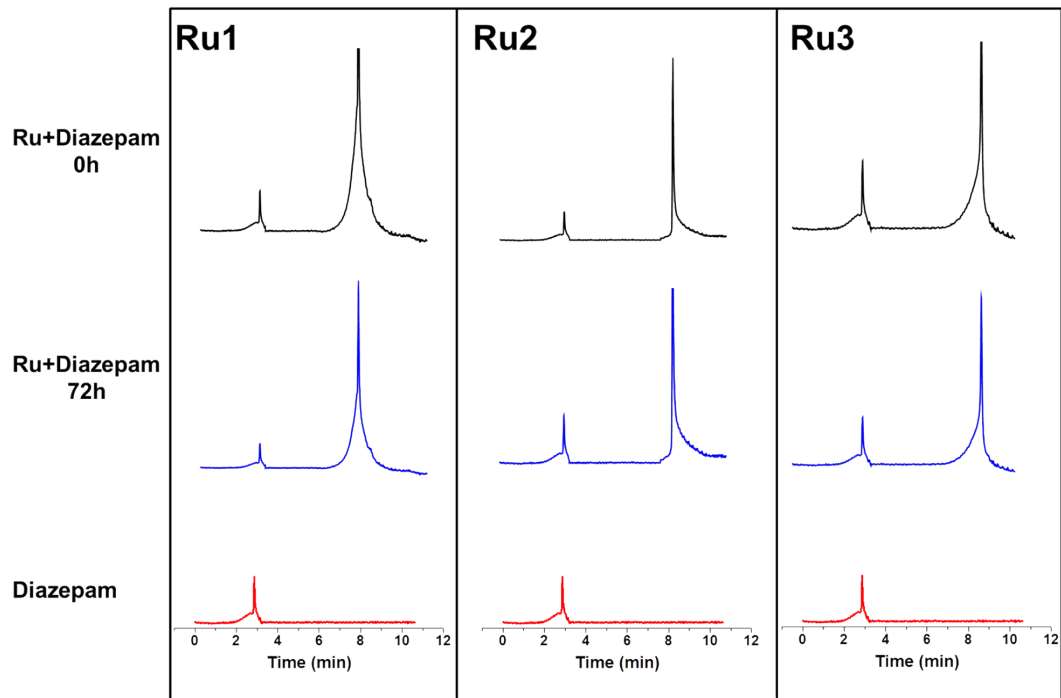


Figure S18 Plasma stability of **Ru1-Ru3** (10 μ M) detected by HPLC.

Table S1. The crystal data and structure detail of **Ru1**.

	Ru1
Empirical formula	C ₃₇ H ₂₅ Cl ₂ N ₉ O ₈ Ru
Formula weight	895.63
Crystal system	Triclinic
Space group	P-1
<i>a</i> / Å	9.0843(17)
<i>b</i> / Å	10.6661(19)
<i>c</i> / Å	22.980(4)
α [°]	94.141(3)
β [°]	98.605(3)
γ [°]	107.719(3)
<i>V</i> [Å ³]	2080.7(6)
Temperature / K	173(2)
<i>Z</i>	2
Data / restraints / parameters	8831 / 18 / 514
R ₁ [$I > 2\sigma(I)$]	0.0493
Final <i>wR</i> (<i>F</i> 2) values ($I > 2\sigma(I)$)	0.1348
Final <i>R</i> _{<i>I</i>} values (all data)	0.0628
<i>wR</i> ₂ (all data)	0.1422

Table S2 Selected bond lengths (Å) and angles (°) for **Ru1**.

Complex	Ru1
Bond length (Å)	Ru(1)-N(2) 2.026(3)
	Ru(1)-N(4) 2.080(3)
	Ru(1)-N(6) 2.056(3)
	Ru(1)-N(7) 1.964(3)
	Ru(1)-N(8) 2.079(3)
	Ru(1)-N(9) 2.105(3)
Bond angles (°)	N(7)-Ru(1)-N(2) 92.45(11)
	N(7)-Ru(1)-N(6) 79.69(13)
	N(2)-Ru(1)-N(6) 91.97(11)
	N(7)-Ru(1)-N(8) 79.40(13)
	N(2)-Ru(1)-N(8) 92.03(12)
	N(6)-Ru(1)-N(8) 158.86(13)
	N(7)-Ru(1)-N(4) 170.84(11)
	N(2)-Ru(1)-N(4) 78.57(11)
	N(6)-Ru(1)-N(4) 98.60(11)
	N(8)-Ru(1)-N(4) 102.53(11)
	N(7)-Ru(1)-N(9) 90.69(11)
	N(2)-Ru(1)-N(9) 176.30(10)
	N(6)-Ru(1)-N(9) 90.52(11)
	N(8)-Ru(1)-N(9) 86.63(12)
	N(4)-Ru(1)-N(9) 98.35(11)

Table S3. Photophysical properties of **Ru1-Ru3** in CH₃CN.

Complex	Absorption		Emission		
	λ /nm (log ε _{max})	λ /nm	Φ /%	τ _{em} / ns	
Ru1	310 (4.91)	494 (4.18)	675	0.97	43
Ru2	305 (4.95)	481 (4.26)	705	0.86	57
Ru3	308 (4.89)	485 (4.28)	710	1.02	50